20. L. I. Sedov, The Mechanics of Continuous Media [in Russian], Vol. 1, Nauka, Moscow (1976).
21. H. Knoepfel and R. Luppi, "The electrical conductivity of metals at very high temperatures," in: Exploding Wires, Vol. 4, London (1968), p. 233.
22. N. B. Volkov, "An investigation of electrophysical processes occurring in connection with the production of superstrong pulsed magnetic fields," Author's abstract of Candidate's Dissertation, Engineering Sciences, Leningrad Polytechnic Inst. (1978).
23. N. B. Volkov, "A plasma model of the conductivity of metals," Zh. Tekh. Fiz., 49, No. 9 (1979).
24. A. Brin, J. E. Besanson, et al., "Magnetic field compression," in: Proceedings of the Conference on Megagauss Magnetic Field Generation by Explosives and Related Experiments, Euratom, Brussels (1966).
25. C. M. Fowler, W. B. Garn, and R. S. Caird, "Production of very high magnetic fields by implosion," J. Appl. Phys., 31, 588 (1960).
26. A. D. Sakharov, R. Z. Lyudaev, et al., "Magnetic cumulation," Dokl. Akad. Nauk SSSR, 165, No. 1 (1965).
27. G. Lehner, J. G. Linhart, and J. P. Somon, "Limitations on magnetic fields obtained by flux compression," Nucl. Fusion, 4, 362 (1964).
28. F. Herlach, "Megagauss magnetic fields," Reports on Progress in Physics, 31, 341 (1968).
29. H. Knoepfel, Pulsed Magnetic Fields, Elsevier (1970).

POSSIBILITY OF APPLYING ELECTROMAGNETIC ACCELERATORS TO INVESTIGATE PROCESSES OCCURRING IN THE HIGH-VELOCITY COLLISION OF SOLIDS

V. F. Agarkov, A. A. Blokhintsev, S. A. Kalikhman, V. I. Kuznetsov, V. N. Fomakin, and A. A. Tsarev

UDC 538.323:534.2

Experiment on the high-velocity collision of structure specimens with particles of less than a millimeter in size at 1-15-km/sec speeds are necessary for the investigation of material properties by the application of mechanical forces. Promising accelerating apparatus are electromagnetic accelerators that use the powerful action of an electromagnetic field on conductors with current. It turns out to be possible to accelerate cylindrical conductors of less than 1-mm diameter to velocities exceeding 10 km/sec [1] in the regime of separate regulation of the accelerating magnetic field and the current in the conductor.

1. Quite important to the quantitative estimate of high-velocity action is the question of the size of the body being accelerated at the time of the collision. If the current density is less than the limit according to the fusion condition, and the conductor diameter is much less than the equivalent depth of penetration ($\Delta_e = \sqrt{2/\omega\sigma\mu_0}$, where ω is the circular frequency of the discharge current, and σ, μ_0 are the conductivity and magnetic permittivity of the conductor material), then sausage-type instabilities cannot develop [2] and the diameter can be considered constant. The length of the conductor diminishes because of thermal processes at the sites of arc contact with the current-carrying rails during the acceleration. Heating occurs by the current flowing in the conductor (volume source) and because of the heat flux from the electrical contact arc (surface source). An analysis (see Appendix) shows that the combined effect of the volume and surface sources is limited, in practice, to a layer of thickness $2\sqrt{at}$, where a is the coefficient of thermal diffusivity and t is the time. Outside this layer, heat transfer from the contact zone can be neglected and it can be considered that the heating occurs only because of the volume source. We use this assumption to compute the evaporation rate and the diminution rate of the length of the conductor being accelerated because of evaporation. The maximal acceleration time and the corresponding limit velocity according to the heating conditions are determined by the time the conductor achieves a certain minimal size according to the conditions of the experimental investigations. Therefore, the energy balance equation has the form

Kuibyshev and Cheboksary. Translated from Zhurnal Prikladnoi Mekhaniki i Tekhnicheskoi Fiziki, No. 5, pp. 26-31, September-October, 1982. Original article submitted September 2, 1981.

0021-8944/82/2305-0617$07.50

$$q(t) = v_1(t)\left\{\gamma c T_1 + L_0(T_1) - \int_0^t j^2(\tau)\,\rho[T(\tau)]\,d\tau\right\}, \tag{1}$$

where $q(t) = |jU_0'|$ is the specific power of the surface source; j, current density; U_0', equivalent pressure drop near the electrode, which equals U_{0a}' and U_{0c}' for the anode and cathode, respectively [3]; v_1, evaporation rate; T_1, temperature of the evaporation surface; $L_0(T_1)$, specific energy of evaporation; and γ, c, ρ are, respectively, the density, specific heat, and specific resistance of the conductor material.

The integral in the right side of (1) depends on the temperature change in time and should be computed with both the surface and volume sources taken into account. We represent it approximately by the sum of two components

$$\int_0^t j^2\rho[T(\tau)]\,d\tau = \int_0^t j^2\rho_0 \exp\left(\frac{\rho_0\alpha}{c\gamma}\int_0^\tau j^2 dz\right)d\tau + j^2\rho_2(T_1)\frac{2\sqrt{at}}{v_1}, \tag{2}$$

where $\rho_2(T_1) = \rho_{20}[1 + \alpha_2(T_1 - T_2)$ is the specific resistance of the liquid phase on the evaporation front, T_2 is the melting temperature, and ρ_0, α, ρ_{20}, α_2 are, respectively, the initial value of the specific resistance and the temperature coefficient of the resistance of the solid and liquid phases.

The first term in (2) is the energy per unit volume because of heating by just the volume source, the change in the specific resistance is taken into account only under the effect of the volume source, the second term is the energy being liberated by the volume source on the evaporation wave front, where the extent of the front is taken to be equal to the zone of combined influence of the surface and volume sources. After manipulation, we obtain from (2)

$$v_1(t) = \frac{|jU_0'| + 2j^2\rho_2(T_1)\sqrt{at}}{\gamma c T_1 + L_0(T_1) - \frac{c\gamma}{\alpha}\left[\exp\left(\frac{\rho_0\alpha}{c\gamma}\int_0^t j^2 d\tau\right) - 1\right]}. \tag{3}$$

The temperature dependence of the specific evaporation energy has a form in conformity with [4]

$$L_0(T_1) = L_0(1 - T_1/T_3)^{1/2}, \tag{4}$$

where T_3 is the critical temperature.

For the thermal rupture mechanism the evaporation rate follows the surface temperature, always remaining in equilibrium with respect to this temperature. Taking account of the reverse particle flux for the Einstein model of a solid, the expression for the evaporation rate has the form [5]:

$$v_1(T_1) = k(B/T_1)\exp(-T^*/T_1); \tag{5}$$

where $B = 3M\bar{u}/2eR$; $T^* = L_0M/\gamma R$; $\bar{u}$ is the mean sound speed in the solid; M, atomic mass; e, base of natural logarithms; R, universal gas constant; and $k \in [0, 1]$, a constant determined by the reverse particle flux.

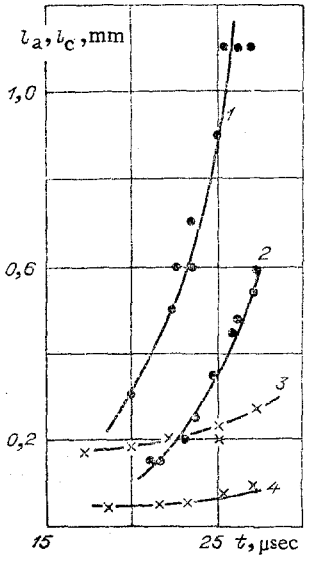

Fig. 1

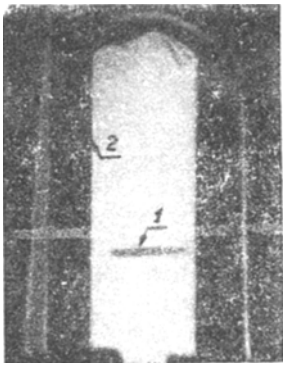

Fig. 2

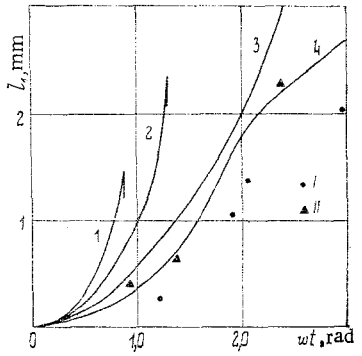

Fig. 3

For known values of the constants and a given current density function, the relationships (3)-(5) form a closed system of equations whose solution for the anode and cathode ends, respectively, of the conductor can determine the total diminution (erosion) of the conductor length because of evaporation:

$$l_1 = \int_0^t (v_{1a} + v_{1c})\, d\tau.$$

In the case being considered of a moving electrical contact arc, the magnitude of the reverse particle flux will depend on both the electrode polarity and the velocity of body displacement. At the anode end the electrical field produces an ion flux from the electrode, while ions are kept at the surface at the cathode end. As the motion velocity increases, the reverse particle flux will diminish, and the value of the coefficient k will tend to unity. To analyze the influence of the polarity and velocity experiments were performed to determine cathode and anode erosion for a fixed and moving conductor. The results of experiments with aluminum conductors (Fig. 1, lines 2 and 4 for the fixed conductor, 1 and 3 conductor moving at the mean velocity 1.8 km/sec, $j = 83 \cdot 10^9 \sin 75.4 \cdot 10^3 t$ $(A/M)_2$, 1 and 2 anode erosion, 3 and 4 cathode erosion) showed that for current densities and times of action characteristic for the high-velocity projectile process, erosion of the cathode end is substantially less than of the anode end in the case of a fixed conductor. Values of the constant for the anode $k_a = 1$ and cathode $k_c = 0.5$ were computed from the experiment results, and which were later assumed unchanged in all the acceleration regimes.

The results of computations on a digital computer by using the method proposed for the case of a sinusoidal change in the current density $j = j_0 \sin \omega t$ were compared with the results of experiments on accleration of conductors. The experiments were performed on the installation ÉMU-1 described in [1]. The erosion was determined by the x-ray diffraction pattern of the conductor being accelerated. A pulse apparatus with a three-electrode tube of "open" type similar to that described in [6] was used for the x-ray diffraction. The photographic film was at a distance less than 15 mm from the conductor, which assured sharpness of the image. Because of the change in the time delay between the beginning of acceleration and the delivery of the pulse to the x-ray tube, x-ray patterns were obtained at different times, including even for collision with an obstacle. A typical x-ray pattern is presented in Fig. 2, where 1 is the conductor and 2 is the current-carrying rail. The magnitude of the erosion can be determined as the difference (taking the scale into account) between the conductor lengths on corresponding x-ray patterns by comparing the pattern for the fixed conductor before the beginning of acceleration and during the motion. The results of computations and experiments for the sinusoidal current case, presented in Fig. 3 (the lines are the computation for aluminum, $U'_{0a} = 19$ V, $U'_{0c} = 9$ V, the experiment results are the points I and II, $j_0 = 70$ and 100 kA/mm^2, $\omega = 157{,}000$ and $220{,}000$ sec^{-1}, respectively, the vertical lines correspond to melting of the conductor under the effect of the volume source; lines 1-4 correspond to $j_0 = 250$, 170, 100, 70 kA/mm^2, 1-3) $\omega = 220{,}000$ sec^{-1}, 4) $\omega = 157{,}000$ sec^{-1} are in good agreement. The system of equations obtained in combination with the equation of motion [1] permits computation of the parameters of a cylindrical body at the time of interaction with an obstacle.

2. Experiments on the high-velocity action of cylindrical bodies on structural materials were performed on the experimental apparatus ÉMU-2 (nominal voltage 50 kV, energy capacity 150 kJ, oscillation frequency 62 kHz). Aluminum wire segments of 4-6 mm initial length (final length 2.3 mm) and 0.2-0.4 mm diameter were used as the body being accelerated. The collision velocity was determined by using SFR-patterning of the acceleration process. Moreover, the maximal possible velocity in the experiment (without taking account of the diminution in magnetic field induction because of thermal and mechanical destruction of the coil) was computed by the oscillograms of the current in the coil and in the conductor being accelerated.

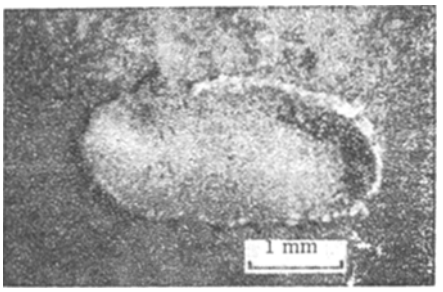

Fig. 4

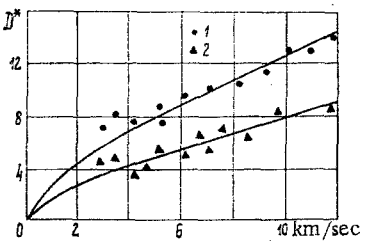

Fig. 5

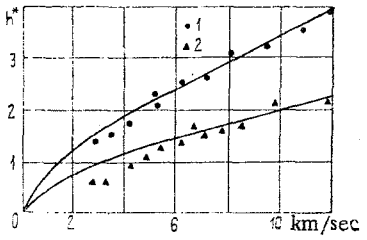

Fig. 6

A photograph of the cavern obtained because of the collision between an aluminum conductor of 0.24-mm diameter at a velocity of 11.3 km/sec with a specimen of M1 copper (the method of measuring the velocity is described in [1]) is presented in Fig. 4. The cavern is oval in shape since the conductor length is much greater than its diameter.

The results of the experiments showed that the length l of a conductor being accelerated influences the cavern parameters as follows: for $l/d_0 \geq 3$, where d_0 is the conductor diameter, the cavern width is practically independent of the conductor length, and the cavern depth diminishes negligibly as the conductor length increases while its diameter remains unchanged.

Dependences of the relative cavern depth h* and width D* on the collision velocity v_0 are constructed according to experimental results for the aluminum alloy AMg6 and copper M1, $h^* = h/d_0$, $D^* = D/d_0$, where h is the absolute value of the cavern depth, and D is the absolute value of the cavern width, and the cavern parameters were measured at the level of the specimen plane.

By analogy with [7], the results of the experiments (Figs. 5 and 6, 1 – AmG6, 2 – M1) were approximated by curves varying according to the law

$$h^* = a_0 \sqrt[3]{v_0^2}, \quad D^* = b_0 \sqrt[3]{v_0^2}, \tag{6}$$

where a_0, b_0 are constant coefficients. The experimental results obtained in the case of cylindrical aluminum impactors for 3-12-km/sec collision velocities agree best with the analytical expressions (6) for values of the approximation coefficients: For specimens from the material AmG6 – $a_0 = 0.75$ $(\text{sec/m})^{2/3}$, $b_0 = 2.75$ $(\text{sec/m})^{2/3}$, from copper M1 – $a_0 = 0.45$ $(\text{sec/m})^{2/3}$, $b_0 = 1.7$ $(\text{sec/m})^{2/3}$.

Therefore, the analytical expressions (6) with appropriate values of the approximation coefficients can be used for both spherical [7] and cylindrical impactors.

By using electromagnetic accelerators of conductors, the modeling of a collision between structural materials and compact bodies of cylindrical shape is possible for velocities exceeding 10 km/sec. For velocities greater than 3 km/sec and the conductor length $l > 3d_0$ extension of the results of collisions with cylindrical bodies to spherical impactors is possible by converting the approximate coefficients a_0 and b_0.

APPENDIX

To examine the combined action of surface and volume sources, we first find the temperature field without taking account of conductor evaporation. Considering the temperature one-dimensional and neglecting heat exchange with the environment, we write the heat-conduction equation and boundary conditions in the form

$$\partial T/\partial t = a\partial^2 T/\partial x^2 + (w_0/c\gamma)(1 + \alpha T); \tag{A1}$$

$$q = \lambda \partial T(l, t)/\partial t, \tag{A2}$$

where $w_0 = j^2\rho$, $q = |jU_0^*|$ are, respectively, the volume and surface source powers; j, current density; ρ_0, initial value of the specific resistance; U_0^*, equivalent near-electrode voltage drop; α, temperature coefficient of resistivity; c, γ, a, and λ, respectively, the specific heat, density, thermal diffusivity, and heat conduction; l, coordinate of the conductor boundary.

To eliminate differential operations with respect to the time, we apply the Laplace integral transform to (A1) and (A2) [8]. Then the transformed equation for the transforms has the following form in the case of constancy of the current density:

$$d^2\tilde{T}(s)/dx^2 + \tilde{T}(s)(w_0\alpha/\lambda - s/a) + w_0/s\lambda + T_0/\alpha = 0. \tag{A3}$$

The solution of (A3) that is symmetric relative to the origin and with the boundary condition taken into account has the form

$$\tilde{T} = \frac{q\,\mathrm{ch}\left(x\sqrt{\frac{s}{a} - \frac{w_0\alpha}{\lambda}}\right)}{s\lambda\sqrt{\frac{s}{a} - \frac{w_0\alpha}{\lambda}}\,\mathrm{sh}\left(l\sqrt{\frac{s}{a} - \frac{w_0\alpha}{\lambda}}\right)} + \frac{w_0}{s\lambda\left(\frac{s}{a} - \frac{w_0\alpha}{\lambda}\right)} + \frac{T_0}{s - \frac{w_0\alpha}{\lambda}}.$$

We apply the inverse Laplace transform to (A4). Making the change of variable $p = s - a_1$ and expanding the function $[\sinh(b_1\sqrt{p})]^{-1}$ in a series of exponential functions [8], we obtain by using the convolution theorem

$$T(x, t) = \frac{q\sqrt{a}}{\lambda}\int_0^t \frac{\exp(a_1\tau)}{\sqrt{\pi\tau}}\sum_{n=1}^{\infty}\left\{\exp\left[-\frac{((2n-1)\,l - x)^2}{4a\tau}\right] + \exp\left[-\frac{((2n-1)\,l + x)^2}{4a\tau}\right]\right\}d\tau + \frac{1}{\alpha}[\exp(a_1 t) - 1] + T_0\exp(a_1 t), \tag{A5}$$

where $a_1 = w_0\alpha/c\gamma$, $b_1 = l/\sqrt{a}$.

The first term in (A5) determines the combined action of the surface and volume heat sources. Computations for parameters characteristic for the process of conductor acceleration in a pulsed magnetic field show that the zone of combined influence can be taken equal to $2\sqrt{at}$ with an acceptable error (10-20%) for computations of the acceleration regime.

LITERATURE CITED

1. V. F. Agarkov, V. N. Bondaletov, et al., "Acceleration of conductors to hypersonic velocities in a pulsed magnetic field," Zh. Prikl. Mekh. Tekh. Fiz., No. 3 (1974).
2. K. B. Abramova, N. A. Zlatin, and B. P. Peregud, "Magnetohydrodynamic instabilities of liquid and solid conductors. Destruction of conductors by an electric current," Zh. Eksp. Teor. Fiz., 69, No. 6(12) (1975).
3. G. V. Butkevich, G. S. Belin, N. A. Vedeshenkov, and M. A. Zharovonkov, Electrical Erosion of High-Current Contacts and Electrodes [in Russian], Énergiya, Moscow (1978).
4. Yu. V. Afanas'ev and O. N. Krokhin, "High-temperature and plasma phenomena occurring during interaction between powerful laser radiation and a substance," in: Physics of High Energy Densities [Russian translation], Mir, Moscow (1974).
5. S. I. Anisimov, Ya. A. Imas, G. S. Romanov, and Yu. V. Khodyko, Action of High Power Radiation on Metals [in Russian], Nauka, Moscow (1970).
6. N. A. Zlatin, A. P. Krasil'shchikov, G. I. Mishin, and N. N. Popov, Ballistic Installations and Their Application in Experimental Investigations [in Russian], Nauka, Moscow (1974).
7. J. Gering, "High-velocity impact from the engineering viewpoint," High-Velocity Impact Phenomena [Russian translation], Mir, Moscow (1973).
8. A. V. Lykov, Theory of Heat Conduction [in Russian], Vysshaya Shkola, Moscow (1967).